5-4-2021

# Comprehensive Molecular and Clinicopathologic Analysis of 200 Pulmonary Invasive Mucinous Adenocarcinomas Identifies Distinct Characteristics of Molecular Subtypes

Jason C. Chang

Michael Offin

Christina Falcon

David Brown

Brian R. Houck-Loomis

*See next page for additional authors*



## Recommended Citation

Chang JC, Offin M, Falcon C, Brown D, Houck-Loomis BR, Meng F, Rudneva VA, Won HH, Amir S, Montecalvo J, Desmeules P, Kadota K, Adusumilli PS, Rusch VW, Teed S, Sabari JK, Benayed R, Nafa K, Borsu L, Li BT, Schram AM, Arcila ME, Travis WD, Ladanyi M, Drilon A, and Rekhtman N. Comprehensive Molecular and Clinicopathologic Analysis of 200 Pulmonary Invasive Mucinous Adenocarcinomas Identifies Distinct Characteristics of Molecular Subtypes. Clin Cancer Res 2021.

## Authors

Jason C. Chang, Michael Offin, Christina Falcon, David Brown, Brian R. Houck-Loomis, Fanli Meng, Vasilisa A Rudneva, Helen H. Won, Sharon Amir, Joseph Montecalvo, Patrice Desmeules, Kyuichi Kadota, Prasad S. Adusumilli, Valerie W. Rusch, Sarah Teed, Joshua K. Sabari, Ryma Benayed, Khedoudja Nafa, Laetitia Borsu, Bob T. Li, Alison M. Schram, Maria E. Arcila, William D. Travis, Marc Ladanyi, Alexander Drilon, and Natasha Rekhtman

Published OnlineFirst May 4, 2021; DOI: 10.1158/1078-0432.CCR-21-0423



# Comprehensive Molecular and Clinicopathologic Analysis of 200 Pulmonary Invasive Mucinous Adenocarcinomas Identifies Distinct Characteristics of Molecular Subtypes

Jason C. Chang[1], Michael Offin[2], Christina Falcon[2], David Brown[3], Brian R. Houck-Loomis[3], Fanli Meng[3], Vasilisa A. Rudneva[3], Helen H. Won[3], Sharon Amir[2], Joseph Montecalvo[1], Patrice Desmeules[1], Kyuichi Kadota[1,4], Prasad S. Adusumilli[4], Valerie W. Rusch[4], Sarah Teed[1,5], Joshua K. Sabari[1], Ryma Benayed[1], Khedoudja Nafa[1], Laetitia Borsu[1], Bob T. Li[2], Alison M. Schram[2], Maria E. Arcila[1], William D. Travis[1], Marc Ladanyi[1,6], Alexander Drilon[2,7], and Natasha Rekhtman[1]

## ABSTRACT

**Purpose:** Invasive mucinous adenocarcinoma (IMA) is a unique subtype of lung adenocarcinoma, characterized genomically by frequent *KRAS* mutations or specific gene fusions, most commonly involving *NRG1*. Comprehensive analysis of a large series of IMAs using broad DNA- and RNA-sequencing methods is still lacking, and it remains unclear whether molecular subtypes of IMA differ clinicopathologically.

**Experimental Design:** A total of 200 IMAs were analyzed by 410-gene DNA next-generation sequencing (MSK-IMPACT; $n = 136$) or hotspot 8-oncogene genotyping ($n = 64$). Driver-negative cases were further analyzed by 62-gene RNA sequencing (MSK-Fusion) and those lacking fusions were further tested by whole-exome sequencing and whole-transcriptome sequencing (WTS).

**Results:** Combined MSK-IMPACT and MSK-Fusion testing identified mutually exclusive driver alterations in 96% of IMAs, including *KRAS* mutations (76%), *NRG1* fusions (7%), *ERBB2* alterations (6%), and other less common events. In addition, WTS identified a novel *NRG2* fusion (*F11R–NRG2*). Overall, targetable gene fusions were identified in 51% of *KRAS* wild-type IMAs, leading to durable responses to targeted therapy in some patients. Compared with *KRAS*-mutant IMAs, *NRG1*-rearranged tumors exhibited several more aggressive characteristics, including worse recurrence-free survival ($P < 0.0001$).

**Conclusions:** This is the largest molecular study of IMAs to date, where we demonstrate the presence of a major oncogenic driver in nearly all cases. This study is the first to document more aggressive characteristics of *NRG1*-rearranged IMAs, *ERBB2* as the third most common alteration, and a novel *NRG2* fusion in these tumors. Comprehensive molecular testing of *KRAS* wild-type IMAs that includes fusion testing is essential, given the high prevalence of alterations with established and investigational targeted therapies in this subset.

[1]Department of Pathology, Memorial Sloan Kettering Cancer Center, New York, New York. [2]Department of Medicine, Thoracic Oncology Service, Memorial Sloan Kettering Cancer Center, New York, New York. [3]Center for Molecular Oncology, Memorial Sloan Kettering Cancer Center, New York, New York. [4]Department of Surgery, Thoracic Service, Memorial Sloan Kettering Cancer Center, New York, New York. [5]Department of Cell Biology, Memorial Sloan Kettering Cancer Center, New York, New York. [6]Human Oncology and Pathogenesis Program, Memorial Sloan Kettering Cancer Center, New York, New York. [7]Department of Medicine, Early Drug Development Service, Memorial Sloan Kettering Cancer Center, New York, New York.

**Note:** Supplementary data for this article are available at Clinical Cancer Research Online (http://clincancerres.aacrjournals.org/).

Current address for J. Montecalvo: Department of Pathology, Henry Ford Hospital, Detroit, Michigan; current address for P. Desmeules: Department of Pathology, Quebec Heart and Lung Institute, Quebec City, Quebec, Canada; current address for K. Kadota: Department of Diagnostic Pathology, University Hospital, Faculty of Medicine, Kagawa University, Kagawa, Japan; and current address for J.K. Sabari: Department of Medicine, New York University Langone Medical Center, New York, New York.

A. Drilon and N. Rekhtman contributed equally as the co-senior authors of this article.

**Corresponding Author:** Natasha Rekhtman, Memorial Sloan Kettering Cancer Center, 1275 York Avenue, New York, NY, 10065. E-mail: rekhtman@mskcc.org

Clin Cancer Res 2021;XX:XX–XX

**doi:** 10.1158/1078-0432.CCR-21-0423



## Introduction

Invasive mucinous adenocarcinoma (IMA), formerly known as mucinous bronchioloalveolar carcinoma, is a unique subtype of primary lung adenocarcinoma, comprising approximately 3%–5% of adenocarcinomas overall (1, 2), with distinct clinical, radiologic, histopathologic, and molecular features. Clinically and radiologically, patients with IMAs commonly present with multifocal and multilobar consolidation, frequently raising the differential diagnosis of pneumonia at the initial presentation (1, 3, 4). Histologically, IMAs are characterized by columnar or goblet-cell morphology with abundant apical intracytoplasmic mucin, basally oriented nuclei and frequent skip lesions (1, 2). Genomically, prior studies showed that *KRAS* mutations are reported in 50%–70% of IMAs (3, 5–8). In those lacking *KRAS* mutations, recent studies revealed the presence of oncogenic fusions in a subset of cases, most commonly involving *NRG1* (5, 6, 9). However, despite further attempts at interrogating *KRAS* wild-type cases using whole-transcriptome sequencing (WTS; ref. 5) or anchored multiplex PCR (6), previous studies failed to reveal a mitogenic driver alteration in the majority of such cases. Notably, the early studies frequently used molecular techniques with limited analytical sensitivity for *KRAS* mutation detection (3, 7, 8), and more recent studies using next-generation sequencing (NGS) techniques only examined mutations and fusions, but not copy-number alterations (5, 6, 10).

Because prior studies have shown limited survival benefits in patients with IMAs treated with conventional chemotherapy (11, 12),

Published OnlineFirst May 4, 2021; DOI: 10.1158/1078-0432.CCR-21-0423



## Translational Relevance

Pulmonary invasive mucinous adenocarcinoma (IMA) is a unique subtype of lung adenocarcinoma, characterized by distinct clinicopathologic and genomic features. This is the largest study to date to use comprehensive DNA- and RNA-based next-generation sequencing to systematically examine the molecular landscape of IMAs. This approach led to identification of an oncogenic driver alteration in nearly all cases. Notably, among *KRAS* wild-type IMAs, *NRG1* and other fusions were identified in over half of the cases and led to durable responses to targeted therapies in some patients. We also describe the distribution of other mutually exclusive and potentially targetable alterations in IMAs and identify distinct histologic and clinical features of molecular subsets. Given the ineffectiveness of traditional cytotoxic approaches and high prevalence of alterations with established or investigational targeted therapies among *KRAS* wild-type IMAs, comprehensive DNA and RNA testing should be considered in such tumors to allow for genome-directed therapies tailored to individual patients.

the quest for more comprehensive characterization of the molecular landscape of IMAs has garnered significant interest, given the targetable nature of many gene fusions. In addition, due to the relative rarity of cases harboring gene fusions such as *NRG1*, the clinicopathologic features of such cases are not well established. Here, we used a combination of sensitive and complementary targeted DNA- and RNA-based molecular assays used in our clinical practice, which included fusion and copy-number alteration analysis, as well as whole-exome sequencing (WES) and WTS for cases lacking a mitogenic driver, in conjunction with detailed morphologic and clinicopathologic analysis to characterize the molecular landscape and compare molecular subsets in a large cohort of IMAs.

## Materials and Methods

### Sample selection and study design

The study was performed with the approval of Institutional Review Board of Memorial Sloan Kettering Cancer Center (MSKCC). Inclusion criteria for the patient cohort were pathologic diagnosis of IMA between 2009 and 2019 for which the patients consented to molecular testing. As summarized in a consort diagram (Supplementary Fig. S1), the study included cases analyzed by two strategies. In the first cohort (diagnosed between 2009 and 2014), we identified 64 IMAs that had undergone hotspot mutation testing by Matrix-assisted laser desorption/ionization-time of flight mass spectrometry (MALDI-TOF MS; ref 13). Cases that were negative for *KRAS* mutations by MALDI-TOF MS underwent high-sensitivity Sanger sequencing with locked nucleic acid (LNA) PCR clamping for enhanced detection of *KRAS* mutations, as previously described (13, 14). *KRAS* wild-type cases were further tested by targeted RNA sequencing (MSK-Fusion) for detection of transcript fusions. In the second cohort (diagnosed between 2014 and 2019), we identified 136 IMAs that underwent targeted DNA sequencing by Memorial Sloan Kettering Integrated Mutation Profiling of Actionable Cancer Targets (MSK-IMPACT) platform. Cases lacking mitogenic driver alterations by MSK-IMPACT also subsequently underwent MSK-Fusion testing. Cases lacking driver alterations after MSK-IMPACT and MSK-Fusion underwent further investigational testing by WES and WTS, as detailed below. Patients with insufficient tumor specimen for complete molecular analysis were excluded.

### Hotspot mutation testing by MALDI-TOF MS

Samples were tested in duplicate using a series of multiplexed assays designed to detect 92 hotspot mutations in eight genes: *EGFR, KRAS, BRAF, PIK3CA, NRAS, AKT1, ERBB2*, and *MAP2K1* (Supplementary Table S1). Genomic DNA amplification and single base pair extension steps were performed using specific primers designed with the Sequenom Assay Designer v3.1 software (Agena BioScience). The allele-specific single base extension products were quantitatively analyzed using MALDI-TOF MS on the Sequenom Mass Array Spectrometer.

### Targeted DNA sequencing by MSK-IMPACT

Broad-panel targeted NGS of patient-matched tumor/normal samples was performed using the MSK-IMPACT assay, the methodology of which has been previously described (15). In brief, the MSK-IMPACT assay is a custom hybridization capture-based platform that sequences the entire coding region and select noncoding regions of 410 (v4) or 468 (v5) genes (full list in Supplementary Table S2) and identifies single-nucleotide variants, small indels, copy-number alterations, and selected structural rearrangements. Germline variants were bioinformatically filtered out based on the matched germline DNA. Manual review of *KRAS* codons 12, 13, and 61 for mutations below the variant allele frequency (VAF) threshold for calling was performed in cases lacking a driver alteration using Integrated Genomics Viewer (16).

### Targeted RNA sequencing by MSK-Fusion

For anchored multiplex RNA sequencing (ArcherDx), the detailed procedure has been previously described (17). Unidirectional gene-specific primers were designed to target specific exons in 62 genes known to be involved in oncogenic fusions in solid tumors (Supplementary Table S3). RNA was extracted from FFPE, followed by complementary DNA synthesis and library preparation. Each RNA sample was tested using the Archer PreSeq RNA QC Assay, a qPCR-based method to assess RNA quality, before library preparation and sequencing. Three samples had $C_t$ values >28, indicating low-quality RNA, and the samples were deemed insufficient for testing and were excluded from the study. Anchored multiplex PCR amplicons were sequenced on an Illumina Miseq sequencer (Illumina), and the data were analyzed using Archer software (ArcherDx).

### WES and analysis

Tumor samples lacking a mitogenic driver alteration by MSK-IMPACT and MSK-Fusion underwent WES with matched normal control. For details, please see Supplementary Method S1.

### WTS and analysis

Tumor samples lacking a mitogenic driver alteration by MSK-IMPACT and MSK-Fusion were also analyzed by WTS. For details, please see Supplementary Method S2.

### Clinical and histologic review

Electronic medical records were reviewed to retrieve relevant clinical data, including patient demographics, smoking and treatment history, and survival outcomes. The primary tumor size was measured pathologically in resected tumors and radiologically in unresectable tumors. Staging was performed according to the American Joint Committee on Cancer 8th edition.

The histologic slides from 200 IMAs were reviewed by two thoracic pathologists (J.C. Chang and N. Rekhtman) using the diagnostic criteria of the 2015 World Health Organization classification. Tumors were classified as pure IMA (entirely mucinous) or mixed IMAs (containing both mucinous and >10% of non-mucinous components).

Published OnlineFirst May 4, 2021; DOI: 10.1158/1078-0432.CCR-21-0423



The presence of tumor necrosis and stromal invasion, defined by stromal desmoplasia surrounding invasive glands or nests of tumor cells, were recorded.

### Statistical analysis

Statistical analyses were performed using GraphPad Prism 8 (GraphPad Software). *P* values were computed using $\chi^2$ test and Student *t* test for categorical and continuous variables, respectively. Overall survival (OS) and recurrence-free survival (RFS) were calculated using the Kaplan–Meier approach from the time of procedure to the time of death and disease recurrence, respectively. Patients were otherwise censored at the time of last clinical follow-up. Survival curves were compared using the log-rank tests. The threshold for statistical significance was set at a *P* value of <0.05.

## Results

### Patient demographics

Baseline patient demographics are summarized in Supplementary Table S4. The median age was 68 years (range, 27–92); 61% of patients were women, 33% were never-smokers, and 28% were light smokers (≤15 pack years). The median smoking history was 8 pack years (range, 0–154). Seventy-nine percent of specimens were resections and 21% were biopsies. The baseline clinical stage distribution was as follows: Stage I 53%, Stage II 16%, Stage III 15%, and Stage IV 16%. On histologic review, 83% of IMAs were pure and 17% were mixed.

### Distribution of driver alterations

In the initial cohort of tumors ($n = 64$) analyzed by MALDI-TOF MS for eight major oncogenes, *KRAS* mutations were identified in 47 cases (73%). In five cases, *KRAS* mutations were initially missed by MALDI-TOF MS, but detected by high-sensitivity Sanger sequencing with LNA probes. Subsequent MSK-Fusion on 17 *KRAS* wild-type IMAs identified fusion drivers in eight (47%) cases (**Fig. 1A**). Overall, driver alterations were identified in 86% of cases in this cohort.

The subsequent cohort of tumors ($n = 136$) analyzed by 410-gene MSK-IMPACT followed by MSK-Fusion on cases with unknown mitogenic driver revealed the following mutually exclusive driver alterations: 104 (76%) *KRAS* mutations, 16 (12%) fusions, and 11 (8%) other driver alterations (**Fig. 1B** and **C**; Supplementary Table S5). Overall, driver alterations were detected in 96% of cases in this cohort, with only five cases (4%) remaining with unknown mitogenic driver after combined MSK-IMPACT and MSK-Fusion testing.

### Overall genomic profile of IMAs by MSK-IMPACT

MSK-IMPACT identified an average of 4 mutations (range, 0–15), 0.7 copy-number alterations (range, 0–8), and 0.1 rearrangements (range, 0–1) per case. The mean tumor mutation burden (TMB) was 3.6 mutations per megabase (mt/Mb), which is significantly lower than the mean TMB of 7.4 mt/Mb for patients with non-mucinous lung adenocarcinoma in the MSK-IMPACT database ($P = 0.0001$; refs. 18, 19). The mean depth of coverage of tumor DNA was 710x (range, 281–1,412).

### Distribution of *KRAS* mutations

A total of 151 *KRAS*-mutant IMAs were identified (104 by MSK-IMPACT, 42 by MALDI-TOF MS, and five by Sanger sequencing with LNA probes), comprising most commonly G12D (36%), G12V (32%), and G12C (12%) variants (**Fig. 1D**). Overall, transition mutations (G12D, G12S, and G13D) accounted for 40% of all *KRAS* variants.

### Distribution of gene fusions

Among all tumors tested, gene fusions were identified in a total of 24 IMAs, including 12 (50%) with *NRG1*, 6 (25%) with *ALK*, 2 (8%) with *ROS1*, and 1 each with *ERBB2, NTRK1, FGFR2*, and *FGFR3* (**Fig. 1A** and **B**). Overall, fusions represented the driver alteration in 24/49 of *KRAS* wild-type IMAs (**Fig. 1A** and **B**). Among 16 fusions in the MSK-IMPACT cohort, six cases were only detected by MSK-Fusion; all of these cases involved *NRG1*, with false negatives likely due to the panel design as *NRG1* introns are not captured by MSK-IMPACT due to their large size. All fusions detected by MSK-IMPACT were confirmed by an orthogonal method (MSK-Fusion, FISH, and/or IHC; Supplementary Table S6).

The most common gene partner for *NRG1* fusions involved *CD74* ($n = 6$), followed by *SLC3A2* ($n = 2$), *SDC4* ($n = 2$), *VAMP2* ($n = 1$), and *F11R* ($n = 1$). All of these genes encode a cell surface protein leading to membranous localization of the fusion protein (**Fig. 2D**). The partner gene for *ALK* ($n = 6$) involved *EML4* in five cases and *PLEKHH2* in one case.

### *ERBB2* and other putative driver alterations

Among cases analyzed by MSK-IMPACT, 11 tumors harbored established or putative oncogenic driver alterations that were non-*KRAS* and non-fusion type, which accounted for 34% (11/32) *KRAS* wild-type IMAs. This included *ERBB2* insertion mutations ($n = 4$), *ERBB2* amplifications ($n = 3$), *BRAF* mutations ($n = 3$), and *ERBB3* mutations ($n = 1$). Overall, *ERBB2* alterations (insertions and amplifications) accounted for 22% of *KRAS* wild-type IMAs. All four *ERBB2* insertions were in-frame, including exon 20 Y772_A775dup (AYVM insertion) in-frame insertions involving the kinase domain in three cases, and an exon 17 V658_V659insR insertion involving the transmembrane domain in the fourth case. All three cases with *ERBB2* amplifications represented high-level gene amplifications ranging from 6.3- to 40.2-fold changes (**Fig. 3E**; ref. 20). The three *BRAF* mutations consisted of V600E, K483E, and G469A variants, all of which are predicted to represent pathogenic variants (21). Finally, one IMA harbored concurrent *ERBB3* G284R and D581N mutations, and both variants are suggested to represent oncogenic mutations (22).

### Other recurrent genetic alterations

Other commonly altered non-driver genes in IMAs tested by MSK-IMPACT included *NKX2–1* ($n = 33$, 24%), *CDKN2A* ($n = 32$, 24%), *STK11* ($n = 20$, 15%), *TP53* ($n = 18$, 13%), *GNAS* ($n = 14$, 10%), and *SMAD4* ($n = 6$, 4%; **Fig. 1B**). All *NKX2–1* mutations were truncating.

As summarized in Supplementary Table S7, comparison of the distribution of concurrent non-driver alterations in *KRAS*-mutant versus *NRG1*-rearranged IMAs was similar, although there was a trend for lower number of concurrent mutations in *NRG1*-rearranged tumors. Likewise, *NRG1*-rearranged tumors harbored lower TMB than other IMAs (1.9 vs. 4.5 mt/Mb, $P = 0.016$ for *NRG1* vs. *KRAS*, respectively).

### WES and WTS on tumors lacking a mitogenic driver

Five IMAs remained with unknown mitogenic driver after MSK-IMPACT and MSK-Fusion testing. These cases were further interrogated by WES and WTS. WES did not identify any additional pathogenic alterations (Supplementary Table S8). Conversely, WTS revealed an in-frame *F11R–NRG2* fusion in one case (**Fig. 2E** and **F**; Supplementary Fig. S2), and an *STK11* out-of-frame fusion in another case (Supplementary Tables S9 and S10).

Published OnlineFirst May 4, 2021; DOI: 10.1158/1078-0432.CCR-21-0423



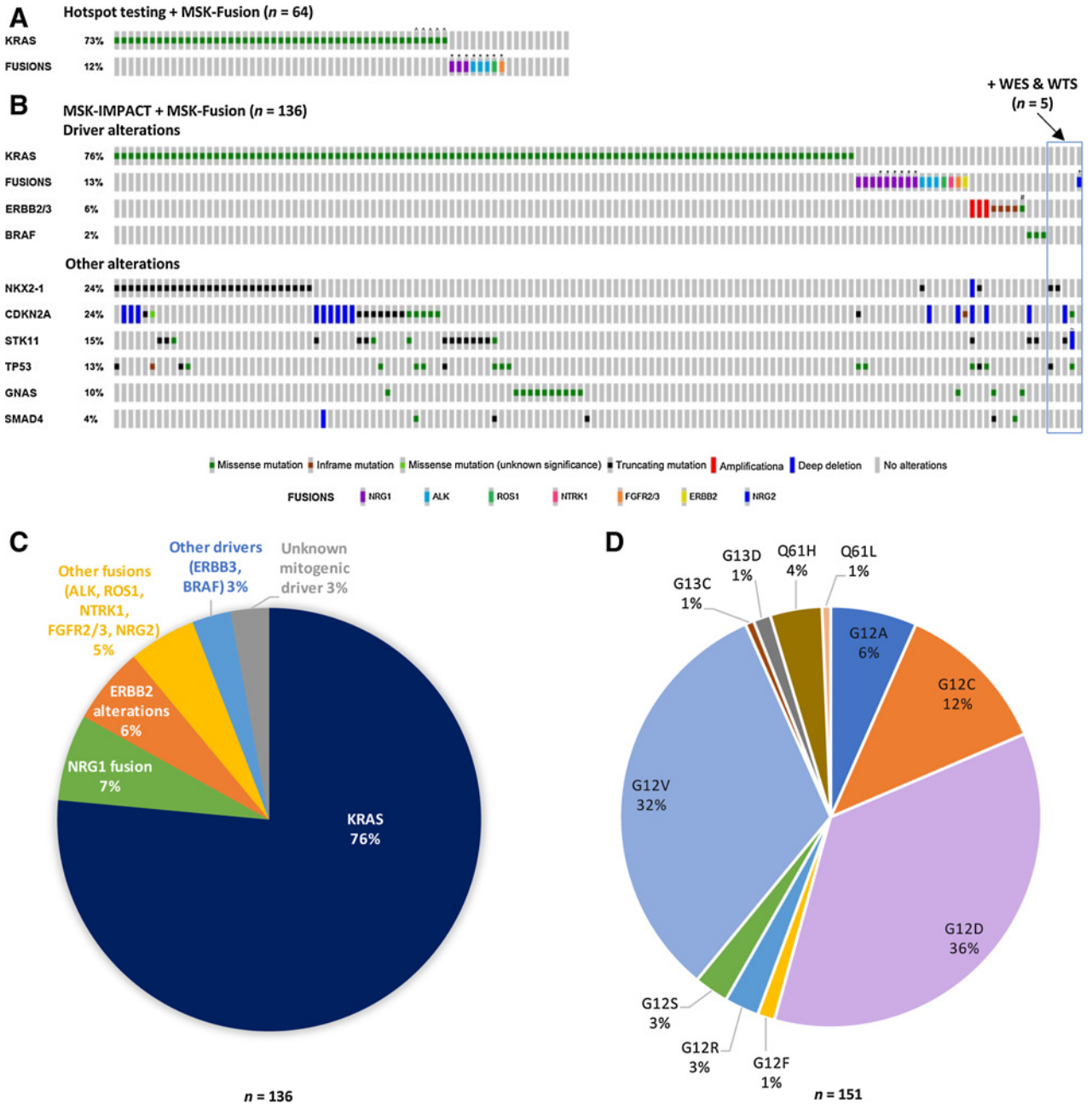


**Figure 1.**

**A,** OncoPrint depicting driver alterations in non-NGS IMA cohort. **B,** OncoPrint depicting driver alterations and other genetic alterations in NGS IMA cohort. **C,** Pie chart summarizing the major classes of driver alterations in NGS IMA cohort ($n = 136$). **D,** Pie chart depicting the subtypes of *KRAS* mutations across *KRAS*-mutant IMAs in both NGS and non-NGS cohort ($n = 151$). ∧, *KRAS* mutations not identified by MALDI-TOF MS and only detected by high-sensitivity Sanger sequencing with LNA probes. *, Fusion genes not identified by MSK-IMPACT and only detected by MSK-Fusion. #, The case harboring concurrent *ERBB3* G284R and D581N mutations. +, The case with *NRG2* fusion detected by whole-transcriptome sequencing. ∼, The case with STK11 truncating fusion detected by whole-transcriptome sequencing.

### Comparison of clinicopathologic features between molecular subsets

As summarized in **Table 1**, comparison of clinicopathologic characteristics between *NRG1*-rearranged and *KRAS*-mutant IMAs revealed that *NRG1* fusions were associated with lower cigarette exposure (mean 5.9 vs. 20 pack years, $P = 0.040$). Furthermore, compared with *KRAS* mutations, *NRG1* fusions were associated with significantly larger primary tumor size (mean 7.7 vs. 3.9 cm, $P = 0.0004$) and significantly higher rate of metastasis overall ($P = 0.016$), particularly extrathoracic metastasis (50% vs. 5%, $P = 0.0006$). Furthermore, survival analysis revealed that compared with *KRAS* mutations, *NRG1* fusions were associated with significantly worse OS in the entire cohort of patients ($P = 0.014$), and significantly worse RFS among patients with surgically resected

Published OnlineFirst May 4, 2021; DOI: 10.1158/1078-0432.CCR-21-0423



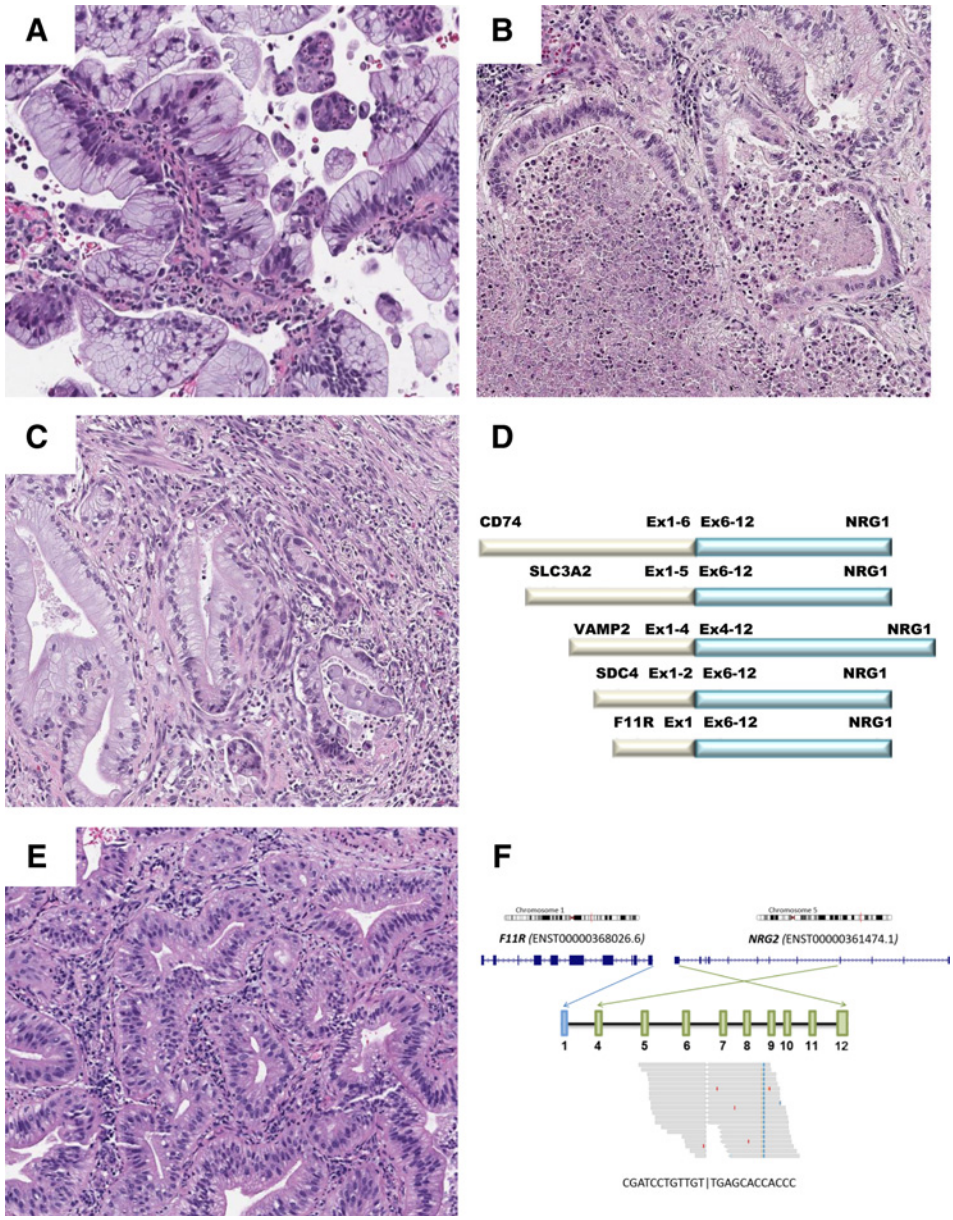


**Figure 2.**

Histologic findings in IMAs with *NRG*1/2 fusions. **A,** This *NRG1*-rearranged carcinoma shows classic mucinous morphology with tall columnar cells, basally located nuclei, and abundant apical cytoplasmic mucin. **B,** Necrosis is a common histologic finding in IMAs with *NRG1* fusions. **C,** A focus of desmoplastic stromal invasion is accompanied by depletion of cytoplasmic mucin. **D,** Structural features of *NRG1* fusions involving the 5′ and 3′ chromosomal partners identified by MSK-Fusion. **E,** This *NRG2*-rearranged tumor is composed of tall columnar cells with pseudostratified nuclei and abundant cytoplasmic mucin. **F,** Schematic illustration of the gene structure and transcript sequence of the *F11R–NRG2* fusion product and representation of complementary DNA sequencing reads supporting the fusion transcript by whole-transcriptome sequencing.

tumors ($P < 0.0001$; **Fig. 4**). Median follow-up was 2.2 years (range, 0.02–16.3 years).

The heterogeneity of *ERBB2* alterations precluded a comparison of survival outcomes based on this aggregated group. However, more aggressive behavior of this subset was supported by the observation that all 3 patients with *ERBB2*-amplified tumors had intrathoracic metastases and died within 1.7–42 months from diagnosis. Likewise, 2 of 4 patients with *ERRB2* insertions had intrathoracic metastases. The clinicopathologic features and survival outcomes of *ERBB2*-altered cases are summarized in Supplementary Table S11.

Analysis of survival characteristics associated with concurrent genomic alterations revealed poorer outcome associated with *TP53* and *CDKN2A* alterations (Supplementary Figs. S3 and S4); multivariable analysis was precluded by small number of patients in molecular subgroups.

Similar to most patients with *NRG1*-rearranged tumors, the single patient with *NRG2*-rearranged IMA was a never-smoker who developed contralateral intrapulmonary metastasis 5 months after initial diagnosis.

## Comparison of histologic features between molecular subsets

Histologically, the prevalence of pure IMA histology was comparable for *NRG1*-rearranged versus *KRAS*-mutant tumors (88% vs. 83%, respectively). However, the presence of aggressive histologic features, including tumor necrosis (**Fig. 2B**) and/or desmoplastic stromal invasion (**Fig. 2C**), was more frequently seen in tumors with *NRG1* fusions compared with *KRAS* mutations (92% vs. 54%, respectively; $P = 0.012$; **Table 1**). Similarly, all cases with *ERBB2* alterations showed pure IMA morphology (**Fig. 3**). In contrast, all cases with *ALK* fusions showed mixed histology.

## Treatment response to targeted therapy

Nine of 30 patients with potentially targetable alterations received targeted therapy; the type of targeted therapy and the best treatment

Published OnlineFirst May 4, 2021; DOI: 10.1158/1078-0432.CCR-21-0423



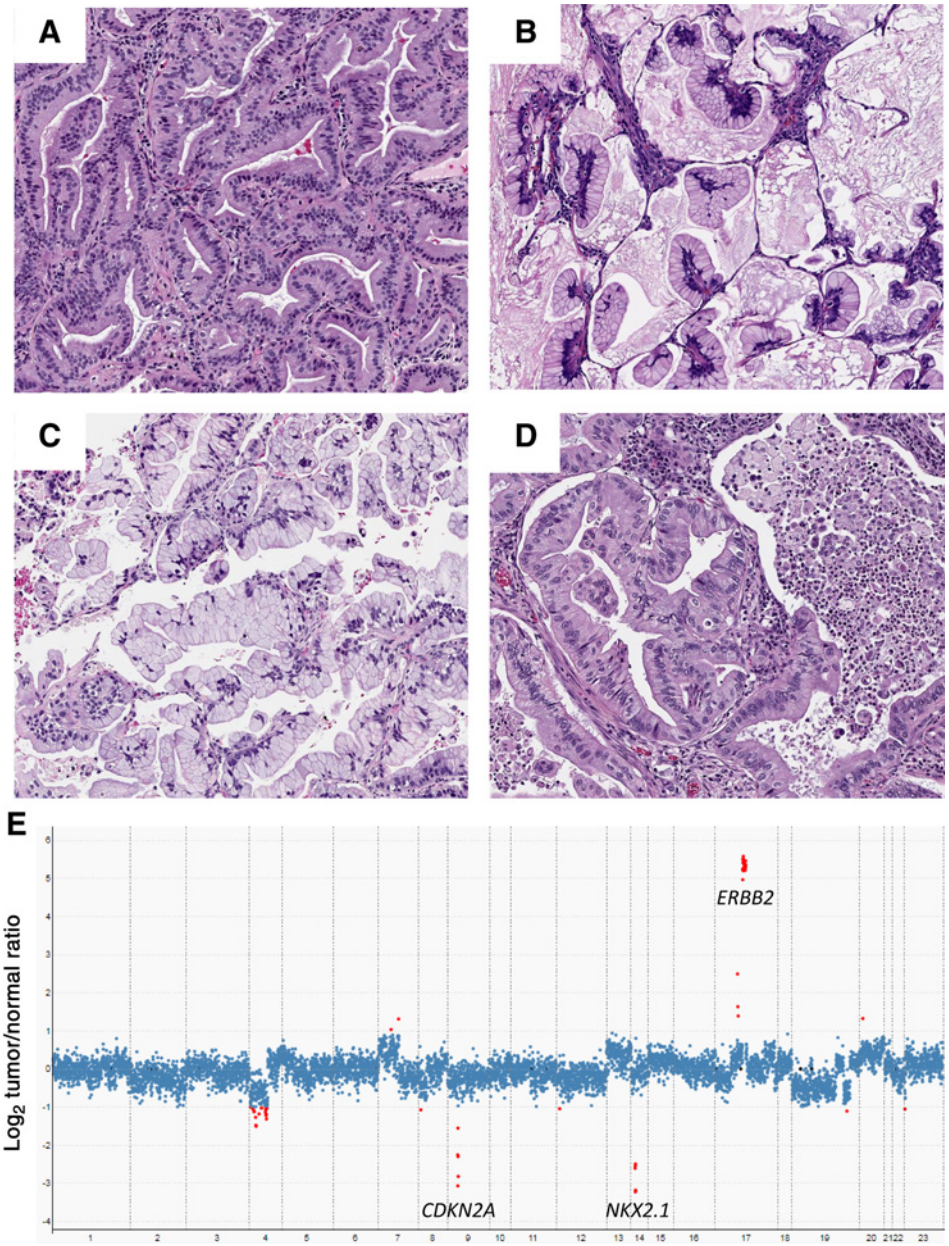


**Figure 3.**
Histologic findings in IMAs with *ERBB2* alterations. **A,** An IMA with *ERBB2* fusion shows classic IMA morphology with tall columnar cells containing abundant apical mucin. **B,** An IMA with *ERBB2* exon 17 insertion mutations shows strips of bland columnar tumor cells in the background of abundant intra-alveolar mucin pools. **C,** An IMA with *ERBB2* amplification shows bland tumor cells with pyknotic basally located nuclei and abundant cytoplasmic mucin. **D,** Another IMA with *ERBB2* amplification shows partially necrotic debris within glandular spaces. **E,** Copy-number plot with relative ($log_2$) tumor/normal ratios (*y* axis) and corresponding chromosomes (*x* axis) in the tumor depicted in **D** demonstrating *ERBB2* amplification (FC, 40.2), *CDKN2A/B* deletion (FC, −4.4), and *NKX2–1* deletion (FC, −7.0). FC, fold change.

response achieved are listed in **Fig. 5**. Of the 5 patients with *NRG1* fusions, 1 showed partial response to anti-ERBB3 mAb (GSK2849330), the details of which were previously reported (23); the remaining 4 patients were treated with afatinib, showing stable disease in 1 and progressive disease in 3. We also reviewed histologic features of 49 patients with *ERBB2*-altered adenocarcinomas in the previously published trial of ERBB2-directed therapies (24), and found that one of them was an IMA with *ERBB2* amplification from the current study. The patient showed a lasting complete response to ado-trastuzumab emtansine.

## Discussion

In this study, we have confirmed and significantly expanded on prior observations that IMAs exhibit unique genomic profiles among lung carcinomas. By a combination of sequential and complementary DNA and RNA testing techniques, we have found that mutually exclusive driver alterations can be identified in the vast majority of IMAs, including *KRAS* mutations (76%), *NRG1* fusions (7% of cases overall and 28% of *KRAS* wild-type tumors), and *ERBB2* alterations (6% of cases overall and 25% of *KRAS* wild-type tumors). In addition, we identify a novel *NRG2* fusion in IMAs by performing WTS on tumors lacking a mitogenic driver by standard clinical methods.

The first major novel finding in this study is that *NRG1*-rearranged (*NRG1*$^+$) IMAs showed distinct clinicopathologic characteristics. The two largest genomic studies on IMAs to date by Nakaoku and colleagues (5) and Shim and colleagues (6) each found *NRG1* fusions to account for 7% of driver alterations in predominantly Asian patient cohorts. However, the clinicopathologic characteristics of *NRG1*$^+$ IMAs were not addressed in detail by these studies. To our knowledge,

Published OnlineFirst May 4, 2021; DOI: 10.1158/1078-0432.CCR-21-0423



**Table 1.** Clinicopathologic comparison of IMAs with *KRAS* mutations, *NRG1* fusions, and other alterations.

| | ***KRAS*** ***N* = 104** | ***NRG1*** ***N* = 12** | **Other** ***N* = 28** | ***P* value for** ***KRAS*$^+$ vs. *NRG1*$^+$** |
|---|---|---|---|---|
| Age at diagnosis (y) | | | | |
| Range | 27–89 | 37–84 | 34–89 | 0.58 |
| Median | 67 | 69 | 62 | |
| Sex | | | | |
| Female | 71 (68%) | 6 (50%) | 14 (50%) | 0.21 |
| Male | 33 (32%) | 6 (50%) | 14 (50%) | |
| Smoking status | | | | |
| Heavy smoker | 41 (39%) | 2 (17%) | 6 (21%) | 0.12 |
| Light smoker (≤15 pack years) | 38 (37%) | 4 (33%) | 8 (29%) | |
| Never | 25 (24%) | 6 (50%) | 14 (50%) | |
| Pack years | | | | |
| Range | 0–120 | 0–43 | 0–80 | 0.040 |
| Mean | 20.0 | 5.9 | 11.3 | |
| Stage at baseline | | | | |
| I | 53 (51%) | 2 (17%) | 11 (39%) | 0.08 |
| II | 23 (22%) | 3 (25%) | 2 (7%) | |
| III | 17 (16%) | 5 (41%) | 6 (22%) | |
| IV | 11 (11%) | 2 (17%) | 9 (32%) | |
| Surgically resected ever | | | | |
| Yes | 92 (88%) | 10 (83%) | 18 (64%) | 0.63 |
| No | 12 (12%) | 2 (17%) | 10 (36%) | |
| Metastatic disease | | | | |
| Yes | 33 (32%) | 8 (67%) | 17 (61%) | 0.016 |
| No | 71 (68%) | 4 (33%) | 11 (39%) | |
| Site of metastasis | | | | |
| Intrathoracic only | 28 (27%) | 2 (17%) | 12 (43%) | 0.0006 |
| Intrathoracic + extrathoracic | 5 (5%) | 6 (50%) | 5 (18%) | |
| Histologic type | | | | |
| Pure IMA | 92 (88%) | 10 (83%) | 13 (46%) | 0.61 |
| Mixed IMA | 12 (12%) | 2 (17%) | 15 (54%) | |
| Primary tumor size, cm | | | | |
| Range | 0.3–19.5 | 2.5–15.5 | 0.4–15.5 | 0.0004 |
| Mean | 3.9 | 7.7 | 5.5 | |
| Aggressive histologic features (tumor necrosis or desmoplastic stromal invasion) | | | | |
| Present | 56 (54%) | 11 (92%) | 17 (61%) | 0.012 |
| Absent | 48 (46%) | 1 (8%) | 11 (39%) | |

this study is the largest one to date to characterize the genomic landscape of IMAs. We found that *NRG1* fusions did not differ in prevalence across ethnicities, as they also accounted for 7% of driver alterations of IMAs in our predominantly Caucasian patient cohort. Although patients with *NRG1*$^+$ tumors exhibited classic IMA morphology, this study reveals that *NRG1* fusions were associated with several distinct characteristics. First, although IMAs in general are enriched in never/light smokers compared with non-mucinous adenocarcinomas (25), patients with *NRG1*$^+$ tumors showed even lower exposure to cigarette smoking compared with those with *KRAS*$^+$ tumors. Second, *NRG1*$^+$ tumors exhibited several more aggressive pathologic characteristics compared with *KRAS*$^+$ tumors, including significantly larger primary tumor size and more aggressive histology in the form of either desmoplastic stromal invasion or tumor necrosis. The presence of these histologic features has been found to correlate with worse prognosis in IMAs in a recently published study (26). Finally, *NRG1*$^+$ tumors had more aggressive clinical behavior manifesting as significantly more frequent extrathoracic metastases and worse OS and RFS than *KRAS*$^+$ tumors. However, the survival analysis is limited by the differences in baseline stage and the relatively small number of *NRG1*$^+$ tumors. Nevertheless, this is the first study to document more aggressive histologic and clinical characteristics of IMAs with *NRG1* fusions.

*NRG1* fusions lead to the expression of chimeric transmembrane proteins, resulting in ERBB3 activation, heterodimerization with ERBB2, and upregulation of the PIK3–AKT signaling pathway (5, 6, 23). In addition to being a major class of driver alterations in IMAs, *NRG1* fusions have also been described in approximately 0.2% of solid tumors overall, including pancreatic, gallbladder, renal, bladder, ovarian, breast, and colorectal cancers (27). The interest in identifying *NRG1* fusions in lung and other tumors is driven by the recent identification of novel therapeutic strategies involving ERBB3-directed therapy that have shown durable responses in patients with advanced tumors harboring this alteration (23, 28, 29). In line with these data, one of the patients with *NRG1* fusions in our study demonstrated sustained clinical responses to ERBB3-directed therapies, supporting specific testing strategies to identify them.

The second major finding is the identification of a novel *F11R–NRG2* fusion in an IMA lacking other mitogenic drivers. To our knowledge, this is the third reported case of lung cancer with an *NRG2* fusion (30, 31), of which one had the identical *F11R* partner gene (31).

Published OnlineFirst May 4, 2021; DOI: 10.1158/1078-0432.CCR-21-0423



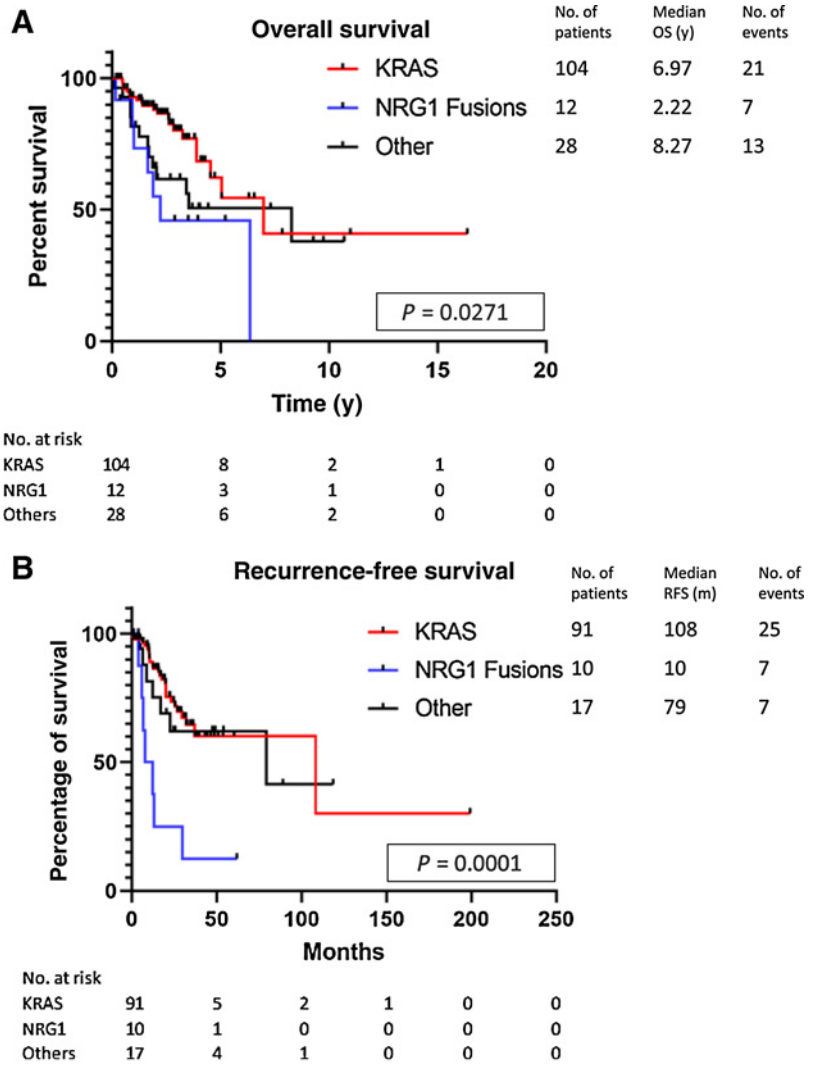


**Figure 4.**
Comparison of overall survival (**A**) and recurrence-free survival (**B**) for IMAs with *KRAS* mutations, *NRG1* fusions, and other driver alterations. The *P* value shown is for three-way comparison. The *P* value for *KRAS* versus *NRG1* is 0.014 (overall survival) and <0.0001 (recurrence-free survival).

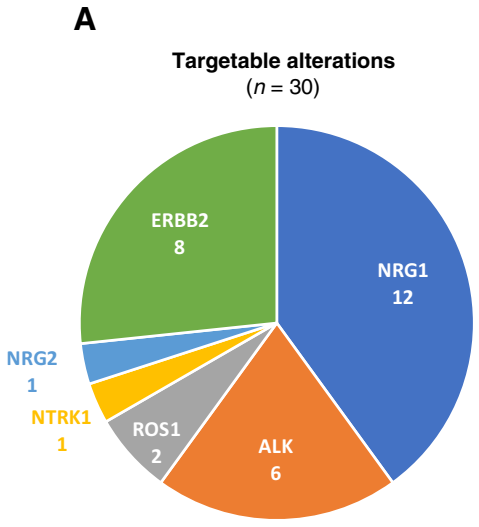


**B** **Clinical benefit of matched targeted therapy** ($n = 9$)

| Alteration | Matched therapy | Best response |
|---|---|---|
| *PLEKHH2-ALK* | Alectinib | SD |
| *EML4-ALK* | Crizotinib | PR |
| *CD74-NRG1* | Afatinib | SD |
| *SDC4-NRG1* | Afatinib | PD |
| *CD74-NRG1* | Afatinib | PD |
| *SLC3A2-NRG1* | Afatinib | PD |
| *CD74-NRG1* | GSK2849330 | PR |
| *CD74-ROS1* | Crizotinib | PD |
| *ERBB2* amplification | Ado-trastuzumab emtansine | CR |

**Figure 5.**
Pie chart summarizing the major classes of targetable alterations in IMAs (**A**) and the best clinical response achieved in patients matched to targeted therapies (**B**). CR, complete response; PD, progressive disease; PR, partial response; SD, stable disease.

Published OnlineFirst May 4, 2021; DOI: 10.1158/1078-0432.CCR-21-0423



The *NRG2* gene encodes a protein that is a homologue of NRG1, which also activates ERBB2/ERBB3 (32). Thus, *NRG2* fusions may be amenable to targeted therapies similar to NRG1 fusions; however, this remains to be confirmed empirically or in experimental models.

We confirmed and further expanded on the spectrum and prevalence of *ERBB2* alterations in IMAs, which represented a recurrent driver in 25% of *KRAS* wild-type IMAs, comprising exon 17 or exon 20 insertion mutations (predominantly Y772_A775dup), amplifications, and fusion. The prior study by Shim and colleagues was the first to describe *ERBB2* Y772_A775dup in two IMAs, in line with our findings. However, to our knowledge, our study was the first to expand the spectrum of *ERBB2* insertions and to identify other types of *ERBB2* alterations (amplifications, fusion) in IMAs, thus establishing *ERBB2* alterations as the third most common putative oncogenic driver in IMAs, following *KRAS* and *NRG1*. Prior studies support that *ERBB2* insertions encountered in IMAs are oncogenic based on molecular modeling (33, 34). The role of *ERBB2* amplification as an oncogenic driver in lung adenocarcinoma is less well established, but is supported by prior studies (35, 36). A previous study from our institution estimated that *ERBB2* insertions and amplifications each accounted for approximately 2% of the driver alterations in lung adenocarcinoma overall, with *ERBB2* exon 20 insertion Y772_A775dup being the most common (33). We retrospectively reviewed lung adenocarcinomas with *ERBB2* insertions and amplifications, and confirmed that they occurred predominantly in conventional, non-mucinous adenocarcinomas (data not shown). Thus, unlike the strong predilection of *NRG1* fusions for IMAs, *ERBB2* alterations are more widely distributed among lung adenocarcinomas. *ERBB2* alterations and *NRG1* fusions are both thought to lead to PIK3–AKT signaling pathway upregulation by increasing homodimerization of ERBB2 and heterodimerization with ERBB3, suggesting downstream signaling convergence. Recently, anti-HER2 therapy has emerged as potential therapeutic agents in lung carcinomas harboring *ERBB2* mutations or amplifications (24, 37, 38). Histologic re-review of patients in the trials revealed that one of the tumors was a classic IMA, and the patient showed a striking sustained complete response to anti-HER2 therapy (24). Similarly, the interim results from the DESTINY-Lung01 trial targeting *ERBB2* alterations indicate promising clinical activity of anti-HER2 therapy (38). Thus, comprehensive molecular testing encompassing various types of *ERBB2* alterations may be warranted in *KRAS* wild-type IMAs.

Although previous studies documented increased likelihood of finding a fusion driver in *KRAS* wild-type IMAs, our study confirmed and further expanded on the prevalence and spectrum of fusion alterations in this subset. In our study, fusions accounted for the driver alterations in 51% of *KRAS* wild-type IMAs, highlighting the utility of incorporating fusion detection in the testing algorithm of IMAs. A recent study from our institution demonstrated that MSK-Fusion identified undetected fusion in 14% of lung adenocarcinomas found to be driver-negative by MSK-IMPACT (39), prompting a recommendation that fusion testing should be considered for all driver-negative lung adenocarcinomas. This recommendation is thus particularly relevant for IMAs. Given that *KRAS* mutations represent the majority of driver alterations in IMAs, for laboratories that do not use upfront comprehensive NGS testing, a high-sensitivity *KRAS* assay may be the appropriate screening test of choice in this tumor type, followed by fusion testing in cases lacking *KRAS* mutations.

Similar to previous studies (5, 6), we found that beyond *NRG1*, the remainder of fusions in IMAs commonly involved one of the receptor tyrosine kinase genes, namely, *ALK, ROS1*, and *NTRK1*. All three fusion genes represent molecular alterations targetable by FDA-approved tyrosine kinase inhibitor therapies. We also described fusions involving *FGFR2* and *FGFR3* in two IMAs—a novel finding for this tumor type. These fusions have been observed in many solid tumors, and rarely in NSCLCs, most commonly squamous cell carcinomas; however, this is the first report of these fusions in IMAs. FGFR inhibitors have been recently approved for use in cholangiocarcinomas; the description of *FGFR2/3* fusions further expanded the list of potentially targetable alterations in IMAs.

Prior studies from our institution have shown that despite similar comprehensive DNA and RNA interrogation, a substantial subset (12%) of conventional lung adenocarcinomas lack a major oncogenic driver (40). Conversely, by similar approaches, a major oncogenic driver is identifiable in the vast majority (97%) of IMAs, emphasizing the unique biology of this ubiquitously driver-associated tumor type. Several factors may underlie the higher prevalence of drivers in our series compared with prior NGS studies of IMAs showing up to 24% of cases without a driver (5, 6, 10). First, the high analytical sensitivity of *KRAS* assays used in this study minimized the chances of false-negative calls, which are frequently encountered in IMAs due to the abundance of mucin and admixed inflammatory cells in this tumor type. This issue was directly observed in this study for five of 47 tumors that initially tested negative for *KRAS* mutations by MALDI-TOF MS, but were subsequently found to be positive for *KRAS* mutations by the more sensitive method. Furthermore, the NGS assay used by the current study was able to detect hotspot mutations in *KRAS* down to 2% VAF. Using these high-sensitivity assays, 76% of IMAs harbored *KRAS* mutations in this cohort, higher than the previously reported prevalence of 50%–63% (7, 8). The second major reason for the low rate of cases with unknown drivers in this cohort is the broad NGS panel incorporating copy-number alteration and fusion detections, supplemented with dedicated fusion testing for all cases lacking a mitogenic driver. This systematic approach using our routine clinical sequencing platforms resulted in the detection of driver alterations in 96% of IMAs. Moreover, using WTS in the research setting detected an additional case with *NRG2* fusion, increasing the overall driver prevalence rate to 97%.

Our findings expand on the prior observations that the molecular profile of IMAs shows close parallels with the genomic landscape of pancreatobiliary adenocarcinomas. This includes the predominance of *KRAS* mutations, as well presence of recurrent alterations in *ERBB2, GNAS*, and *SMAD4* in both tumor types. In addition, the predominance of *KRAS* G12D and G12V variants in IMAs mirrors the distribution of these variants in pancreatic and gastrointestinal adenocarcinomas (41). Conversely, this distribution contrasts sharply with non-mucinous lung adenocarcinomas in the Western population, where *KRAS* G12C represents the most common variant, accounting for approximately 40% of *KRAS* mutations (42), compared with only 12% in IMAs. Despite low prevalence, patients with IMAs harboring *KRAS* G12C mutations may be candidates for *KRAS* G12C inhibitor trials (43). Remarkably, recent studies have shown that *KRAS* wild-type pancreatic adenocarcinomas are also enriched in fusion genes, specifically those involving *NRG1* (27–29).

In summary, our results uncover the high prevalence of mutually exclusive driver alterations in IMAs, comprising most commonly *KRAS* mutations, *NRG1* fusions, and *ERBB2* alterations. We show for the first time that *NRG1*$^{+}$ tumors are associated with aggressive histologic features and worse clinical outcomes. We also identified a novel *NRG2* fusion in this tumor type. As IMAs lacking a mitogenic

driver account for a small minority of cases, comprehensive genomic profiling, including copy-number alteration and fusion detection, should be considered in *KRAS* wild-type IMAs to investigate for the presence of alternative driver events. The description of these alternative driver mechanisms in IMAs offers a rationale for targeted therapeutic strategies with approved and investigational agents for these tumors where traditional cytotoxic approaches are notoriously ineffective.

## Authors' Disclosures

M. Offin reports personal fees from OncLive, PharmaMar, Novartis, Targeted Oncology, and Jazz Pharmaceuticals outside the submitted work. P. Desmeules reports grants and personal fees from Pfizer; grants from Novartis and EMD-Serrono; and grants and personal fees from AstraZeneca and Eli-Lilly outside the submitted work. V.W. Rusch reports grants from NIH during the conduct of the study; V.W. Rusch also reports grants from Genelux Inc. and Genentech, as well as other support from Intuitive Surgical outside the submitted work. J.K. Sabari reports personal fees from AstraZeneca, Genentech Roche, Janssen, Navire, Pfizer, Regeneron, Sanofi Genzyme, and Takeda outside the submitted work. K. Nafa reports other support from Biocartis during the conduct of the study, as well as non-financial support and other support from Biocartis outside the submitted work. B.T. Li reports grants from National Institutes of Health during the conduct of the study. B.T. Li also reports grants and other support from Genentech Roche; grants and personal fees from Guardant Health and Hengrui Therapeutics; grants and other support from Lilly, AstraZeneca, and Daiichi Sankyo; grants from GRAIL; grants and non-financial support from MORE Health; non-financial support and other support from Resolution Bioscience; non-financial support from Jiangsu Hengrui Medicine; personal fees from Boehringer Ingelheim; grants and other support from Bolt Biotherapeutics; and grants from National Institutes of Health outside the submitted work. B.T. Li also reports a patent for US62/685,057 issued, a patent for US62/514,661 issued, a patent for Karger Publishers with royalties paid, and a patent for Shanghai Jiao Tong University Press licensed. A.M. Schram reports other support from Merus outside the submitted work. M.E. Arcila reports personal fees from invivoscribe, biocartis, AztraZeneca, Bristol-Myers Squibb, Clinical Care Options, Janssen Global Services, LLC, and Physicians' Education Resource, LLC outside the submitted work. M. Ladanyi reports grants from Elevation Oncology and Merus, as well as non-financial support from GlaxoSmithKline outside the submitted work. A. Drilon reports personal fees from Ignyta/Genentech/Roche, Loxo/Bayer/Lilly, Takeda/Ariad/Millenium, TP Therapeutics, AstraZeneca, Pfizer, Hengrui Therapeutics, Exelixis, Tyra Biosciences, Verastem, MORE Health, Abbvie, 14ner/Elevation Oncology, Remedica Ltd., ArcherDX, Monopteros, Novartis, EMD Serono, Melendi, Liberum, and Repare RX, as well as other support from GlaxoSmithKline, Teva, Taiho, and PharmaMar outside the submitted work. A. Drilon also reports royalties from Wolters Kluwer; other (food/beverage) from Merck, Puma, Merus, and Boehringer Ingelheim; and CME honoraria from Medscape, OncLive, PeerVoice, Physicians Education Resources, Targeted Oncology, Research to Practice, Axis, PeerView Institute, Paradigm Medical Communications, WebMD, and MJH Life Sciences. No disclosures were reported by the other authors.

## Authors' Contributions

**J.C. Chang:** Conceptualization, resources, data curation, formal analysis, supervision, visualization, methodology, writing–original draft, project administration, writing–review and editing. **M. Offin:** Data curation, formal analysis, writing–original draft, writing–review and editing. **C. Falcon:** Data curation, formal analysis, investigation, visualization, writing–review and editing. **D. Brown:** Formal analysis, visualization, methodology, writing–review and editing. **B.R. Houck-Loomis:** Formal analysis, visualization, methodology, writing–review and editing. **F. Meng:** Formal analysis, methodology, writing–review and editing. **V.A. Rudneva:** Formal analysis, methodology, writing–review and editing. **H.H. Won:** Formal analysis, methodology, writing–review and editing. **S. Amir:** Data curation, formal analysis, writing–review and editing. **J. Montecalvo:** Data curation, writing–review and editing. **P. Desmeules:** Data curation, formal analysis, writing–review and editing. **K. Kadota:** Investigation, writing–review and editing. **P.S. Adusumilli:** Resources, writing–review and editing. **V.W. Rusch:** Resources, writing–review and editing. **S. Teed:** Data curation, writing–review and editing. **J.K. Sabari:** Data curation, writing–review and editing. **R. Benayed:** Investigation, methodology, writing–review and editing. **K. Nafa:** Investigation, methodology, writing–review and editing. **L. Borsu:** Formal analysis, methodology, writing–review and editing. **B.T. Li:** Resources, data curation, writing–review and editing. **A.M. Schram:** Resources, writing–review and editing. **M.E. Arcila:** Formal analysis, validation, investigation, methodology, writing–review and editing. **W.D. Travis:** Resources, supervision, writing–review and editing. **M. Ladanyi:** Formal analysis, validation, investigation, methodology, writing–review and editing. **A. Drilon:** Conceptualization, resources, supervision, funding acquisition, project administration, writing–review and editing. **N. Rekhtman:** Conceptualization, resources, data curation, formal analysis, supervision, funding acquisition, writing–original draft, project administration, writing–review and editing.

## Acknowledgments

We acknowledge the use of the Integrated Genomics Operation Core, funded by the NCI Cancer Center support grant (CCSG, P30 CA08748), Cycle for Survival, and the Marie-Josée and Henry R. Kravis Center for Molecular Oncology. Support was in part by a Memorial Sloan Kettering Cancer Center Department of Pathology Research and Development grant (to N. Rekhtman and J.C. Chang). The MSK-IMPACT program is supported in part by NIH P01 CA129243 (to M. Ladanyi and N. Rekhtman), NIH P30 CA008748 (MSKCC), and the Marie-Josée and Henry R. Kravis Center for Molecular Oncology at MSKCC. The MSKCC Sequenom facility was supported by the Anbinder Fund.

The costs of publication of this article were defrayed in part by the payment of page charges. This article must therefore be hereby marked *advertisement* in accordance with 18 U.S.C. Section 1734 solely to indicate this fact.

Received February 3, 2021; revised March 27, 2021; accepted April 30, 2021; published first May 4, 2021.

## References

1. Travis WD, Brambilla E, Noguchi M, Nicholson AG, Geisinger KR, Yatabe Y, et al. International Association for the Study of Lung Cancer/American Thoracic Society/European Respiratory Society international multidisciplinary classification of lung adenocarcinoma. J Thorac Oncol 2011;6:244–85.
2. Yoshizawa A, Motoi N, Riely GJ, Sima CS, Gerald WL, Kris MG, et al. Impact of proposed IASLC/ATS/ERS classification of lung adenocarcinoma: prognostic subgroups and implications for further revision of staging based on analysis of 514 stage I cases. Mod Pathol 2011;24:653–64.
3. Hata A, Katakami N, Fujita S, Kaji R, Imai Y, Takahashi Y, et al. Frequency of EGFR and KRAS mutations in Japanese patients with lung adenocarcinoma with features of the mucinous subtype of bronchioloalveolar carcinoma. J Thorac Oncol 2010;5:1197–200.
4. Casali C, Rossi G, Marchioni A, Sartori G, Maselli F, Longo L, et al. A single institution-based retrospective study of surgically treated bronchioloalveolar adenocarcinoma of the lung: clinicopathologic analysis, molecular features, and possible pitfalls in routine practice. J Thorac Oncol 2010;5:830–6.
5. Nakaoku T, Tsuta K, Ichikawa H, Shiraishi K, Sakamoto H, Enari M, et al. Druggable oncogene fusions in invasive mucinous lung adenocarcinoma. Clin Cancer Res 2014;20:3087–93.
6. Shim HS, Kenudson M, Zheng Z, Liebers M, Cha YJ, Hoang Q, et al. Unique genetic and survival characteristics of invasive mucinous adenocarcinoma of the lung. J Thorac Oncol 2015;10:1156–62.
7. Ichinokawa H, Ishii G, Nagai K, Kawase A, Yoshida J, Nishimura M, et al. Distinct clinicopathologic characteristics of lung mucinous adenocarcinoma with KRAS mutation. Hum Pathol 2013;44:2636–42.
8. Kakegawa S, Shimizu K, Sugano M, Miyamae Y, Kaira K, Araki T, et al. Clinicopathological features of lung adenocarcinoma with KRAS mutations. Cancer 2011;117:4257–66.
9. Fernandez-Cuesta L, Plenker D, Osada H, Sun R, Menon R, Leenders F, et al. CD74–NRG1 fusions in lung adenocarcinoma. Cancer Discov 2014;4:415–22.
10. Kishikawa S, Hayashi T, Saito T, Takamochi K, Kohsaka S, Sano K, et al. Diffuse expression of MUC6 defines a distinct clinicopathological subset of pulmonary invasive mucinous adenocarcinoma. Mod Pathol 2021;34:786–97.

11. Cha YJ, Kim HR, Lee H-J, Cho BC, Shim HS. Clinical course of stage IV invasive mucinous adenocarcinoma of the lung. Lung Cancer 2016;102:82–8.
12. Cha YJ, Shim HS. Biology of invasive mucinous adenocarcinoma of the lung. Transl Lung Cancer Res 2017;6:508–12.
13. Arcila M, Lau C, Nafa K, Ladanyi M. Detection of KRAS and BRAF mutations in colorectal carcinoma: roles for high-sensitivity locked nucleic acid-PCR sequencing and broad-spectrum mass spectrometry genotyping. J Mol Diagn 2011;13:64–73.
14. Nafa K, Hameed M, Arcila ME. Locked nucleic acid probes (LNA) for enhanced detection of low-level, clinically significant mutations. Methods Mol Biol 2016; 1392:71–82.
15. Zehir A, Benayed R, Shah RH, Syed A, Middha S, Kim HR, et al. Mutational landscape of metastatic cancer revealed from prospective clinical sequencing of 10,000 patients. Nat Med 2017;23:703–13.
16. Robinson JT, Thorvaldsdóttir H, Winckler W, Guttman M, Lander ES, Getz G, et al. Integrative genomics viewer. Nat Biotechnol 2011;29:24–6.
17. Zheng Z, Liebers M, Zhelyazkova B, Cao Y, Panditi D, Lynch KD, et al. Anchored multiplex PCR for targeted next-generation sequencing. Nat Med 2014;20: 1479–84.
18. Cerami E, Gao J, Dogrusoz U, Gross BE, Sumer SO, Aksoy BA, et al. The cBio Cancer Genomics Portal: an open platform for exploring multidimensional cancer genomics data. Cancer Discov 2012;2:401.
19. Gao J, Aksoy BA, Dogrusoz U, Dresdner G, Gross B, Sumer SO, et al. Integrative analysis of complex cancer genomics and clinical profiles using the cBioPortal. Sci Signal 2013;6:pl1.
20. Ross DS, Zehir A, Cheng DT, Benayed R, Nafa K, Hechtman JF, et al. Next-generation assessment of human epidermal growth factor receptor 2 (ERBB2) amplification status: clinical validation in the context of a hybrid capture-based, comprehensive solid tumor genomic profiling assay. J Mol Diagn 2017;19: 244–54.
21. Noeparast A, Teugels E, Giron P, Verschelden G, De Brakeleer S, Decoster L, et al. Non-V600 BRAF mutations recurrently found in lung cancer predict sensitivity to the combination of trametinib and dabrafenib. Oncotarget 2016;8:60094–108.
22. Kiavue N, Cabel L, Melaabi S, Bataillon G, Callens C, Lerebours F, et al. ERBB3 mutations in cancer: biological aspects, prevalence and therapeutics. Oncogene 2020;39:487–502.
23. Drilon A, Somwar R, Mangatt BP, Edgren H, Desmeules P, Ruusulehto A, et al. Response to ERBB3-directed targeted therapy in NRG1-rearranged cancers. Cancer Discov 2018;8:686.
24. Li BT, Michelini F, Misale S, Cocco E, Baldino L, Cai Y, et al. HER2-mediated internalization of cytotoxic agents in ERBB2 amplified or mutant lung cancers. Cancer Discov 2020;10:674.
25. Janjigian YY, McDonnell K, Kris MG, Shen R, Sima CS, Bach PB, et al. Pack-years of cigarette smoking as a prognostic factor in patients with stage IIIB/IV non–small cell lung cancer. Cancer 2010;116:670–5.
26. Chang W-C, Zhang YZ, Lim E, Nicholson AG. Prognostic impact of histopathologic features in pulmonary invasive mucinous adenocarcinomas: proposal for a pathologic grading system. Am J Clin Pathol 2020;154:88–102.
27. Jonna S, Feldman RA, Swensen J, Gatalica Z, Korn WM, Borghaei H, et al. Detection of NRG1 gene fusions in solid tumors. Clin Cancer Res 2019;25:4966.
28. Heining C, Horak P, Uhrig S, Codo PL, Klink B, Hutter B, et al. NRG1 fusions in KRAS wild-type pancreatic cancer. Cancer Discov 2018;8:1087.
29. Jones MR, Williamson LM, Topham JT, Lee MKC, Goytain A, Ho J, et al. NRG1 gene fusions are recurrent, clinically actionable gene rearrangements in KRAS wild-type pancreatic ductal adenocarcinoma. Clin Cancer Res 2019; 25:4674.
30. Kohsaka S, Hayashi T, Nagano M, Ueno T, Kojima S, Kawazu M, et al. Identification of novel CD74-NRG2 fusion from comprehensive profiling of lung adenocarcinoma in Japanese never or light smokers. J Thorac Oncol 2020; 15:948–61.
31. Ou S-HI, Xiu J, Nagasaka M, Xia B, Zhang SS, Zhang Q, et al. Identification of novel CDH1-NRG2α and F11R–NRG2α fusions in NSCLC plus additional novel NRG2α fusions in other solid tumors by whole-transcriptome sequencing. JTO Clin Res Rep 2021;2:100132.
32. Hobbs SS, Coffing SL, Le ATD, Cameron EM, Williams EE, Andrew M, et al. Neuregulin isoforms exhibit distinct patterns of ErbB family receptor activation. Oncogene 2002;21:8442–52.
33. Arcila ME, Chaft JE, Nafa K, Roy-Chowdhuri S, Lau C, Zaidinski M, et al. Prevalence, clinicopathologic associations, and molecular spectrum of ERBB2 (HER2) tyrosine kinase mutations in lung adenocarcinomas. Clin Cancer Res 2012;18:4910–8.
34. Ou SI, Schrock AB, Bocharov EV, Klempner SJ, Haddad CK, Steinecker G, et al. HER2 transmembrane domain (TMD) mutations (V659/G660) that stabilize homo- and heterodimerization are rare oncogenic drivers in lung adenocarcinoma that respond to afatinib. J Thorac Oncol 2017;12:446–57.
35. Collisson EA, Campbell JD, Brooks AN, Berger AH, Lee W, Chmielecki J, et al. Comprehensive molecular profiling of lung adenocarcinoma. Nature 2014;511: 543–50.
36. Li BT, Ross DS, Aisner DL, Chaft JE, Hsu M, Kako SL, et al. HER2 amplification and HER2 mutation are distinct molecular targets in lung cancers. J Thorac Oncol 2016;11:414–9.
37. Li BT, Shen R, Buonocore D, Olah ZT, Ni A, Ginsberg MS, et al. Ado-trastuzumab emtansine for patients with HER2-mutant lung cancers: results from a phase II basket trial. J Clin Oncol 2018;36:2532–7.
38. Smit EF, Nakagawa K, Nagasaka M, Felip E, Goto Y, Li BT, et al. Trastuzumab deruxtecan (T-DXd; DS-8201) in patients with HER2-mutated metastatic non–small cell lung cancer (NSCLC): interim results of DESTINY-Lung01. J Clin Oncol 2020;38:9504.
39. Benayed R, Offin M, Mullaney K, Sukhadia P, Rios K, Desmeules P, et al. High yield of RNA sequencing for targetable kinase fusions in lung adenocarcinomas with no driver alteration detected by DNA sequencing and low tumor mutation burden. Clin Cancer Res 2019;25:4712–22.
40. Jordan EJ, Kim HR, Arcila ME, Barron D, Chakravarty D, Gao J, et al. Prospective comprehensive molecular characterization of lung adenocarcinomas for efficient patient matching to approved and emerging therapies. Cancer Discov 2017;7: 596–609.
41. Bournet B, Muscari F, Buscail C, Assenat E, Barthet M, Hammel P, et al. KRAS G12D mutation subtype is a prognostic factor for advanced pancreatic adenocarcinoma. Clin Transl Gastroenterol 2016;7:e157.
42. Dogan S, Shen R, Ang DC, Johnson ML, Angelo SP, Paik PK, et al. Molecular epidemiology of EGFR and KRAS mutations in 3,026 lung adenocarcinomas: higher susceptibility of women to smoking-related KRAS-mutant cancers. Clin Cancer Res 2012;18:6169.
43. Hong DS, Fakih MG, Strickler JH, Desai J, Durm GA, Shapiro GI, et al. KRAS G12C inhibition with sotorasib in advanced solid tumors. N Engl J Med 2020; 383:1207–17.

AACR American Association for Cancer Research

Clinical Cancer Research

# Comprehensive Molecular and Clinicopathologic Analysis of 200 Pulmonary Invasive Mucinous Adenocarcinomas Identifies Distinct Characteristics of Molecular Subtypes

Jason C. Chang, Michael Offin, Christina Falcon, et al.

*Clin Cancer Res* Published OnlineFirst May 4, 2021.